R&D NOTE

# Application of Distillative Freezing in the Separation of *o*-Xylene and *p*-Xylene

**Lie-Ding Shiau, Chun-Ching Wen, and Bo-Shiue Lin**
Dept. of Chemical and Materials Engineering, Chang Gung University, Taoyuan, Taiwan, Republic of China

*DOI 10.1002/aic.10775*
*Published online January 13, 2006 in Wiley InterScience (www.interscience.wiley.com).*

*Keywords: distillative freezing, separation, purification, o-xylene, p-xylene*

## Introduction

The distillative freezing (DF) operation was first introduced by Cheng and Cheng[1] to separate the mixture of the volatile compounds at a reduced pressure. In principle, the DF process is operated at a triple-point condition in which the liquid mixture is simultaneously vaporized and solidified as a consequence of the three-phase equilibrium. By lowering temperature and reducing pressure during the operation, the DF process results in the formation of pure solid and both liquid and vapor phases of the mixtures. In essence, the DF process is continued until the liquid phase is completely eliminated and only the pure solid crystals remain in the feed. The low-pressure vapor formed in the process is condensed and removed.

Xylenes have very broad applications in chemical industries. The mixed xylenes produced mainly consist of *p*-xylene (PX), *m*-xylene (MX), *o*-xylene (OX), and ethylbenzene (EB). The very close boiling points of theses isomers make it difficult to separate them from each other by conventional distillation. For example, a distillation column of about 150 trays and a high reflux ratio is needed to distill OX from a mixture.[2] Shiau et al.[3] described the basic principle of DF in detail and successfully applied the DF process to produce PX crystals from a liquid mixture of 90% PX and 10% MX. Because the DF process is conducted under an adiabatic condition at a three-phase equilibrium, the latent heat released in crystallization is removed by vaporization. Thus, it is a superlatively energy conserving separation method compared to distillation.[1,3] The objective of this work is to investigate the feasibility of the DF process in separating the binary liquid mixture of OX and PX to produce high-purity chemicals. First, the DF process will be applied to produce PX crystals from the PX-enriched mixture. Second, the DF process will be applied to produce OX crystals from the OX-enriched mixture.

## Principle of the DF Process

Figure 1a illustrates the phase diagram of OX (A-component) and PX (B-component) at $P = 66.66$ Pa, which is lower than the triple-point pressure of pure PX. The construction of Figure 1a, described in detail by Shiau et al.,[3] shows the existence of a three-phase state (point b, point b′, and point b″) having pure B-solid, and both liquid and vapor phases of mixtures at $T = -14.6$°C, $X_B = 0.46$, and $Y_B = 0.56$. Note that the eutectic point lies at $T = -35.3$°C and $X_B = 0.24$, at which both OX and PX crystallize out from the liquid mixture. Some important physical properties for OX and PX are listed in Table 1.

When the DF operation is applied to produce PX crystals from the binary mixture in the range $0.24 < X_B < 1$, the DF process always must be maintained at a three-phase state having pure B-solid, and both liquid and vapor phases of mixtures. Thus, we can derive[4,5]

$$\ln[(X_B)(\gamma_B)] = \frac{\Delta H_{m,B}}{R}\left(\frac{1}{T_{m,B}} - \frac{1}{T}\right) + \frac{\Delta C_{P,B}}{R}\left(\frac{T_{m,B} - T}{T}\right) - \frac{\Delta C_{p,B}}{R}\ln\left(\frac{T_{m,B}}{T}\right) \quad (1)$$

$$P(Y_A)(\phi_A) = (P_A^{sat})(X_A)(\gamma_A) \quad (2)$$

$$P(Y_B)(\phi_B) = (P_B^{sat})(X_B)(\gamma_B) \quad (3)$$

Besides, we have

$$X_A + X_B = 1 \quad (4)$$

$$Y_A + Y_B = 1 \quad (5)$$

Correspondence concerning this article should be addressed to L.-D. Shiau at shiau@mail.cgu.edu.tw.

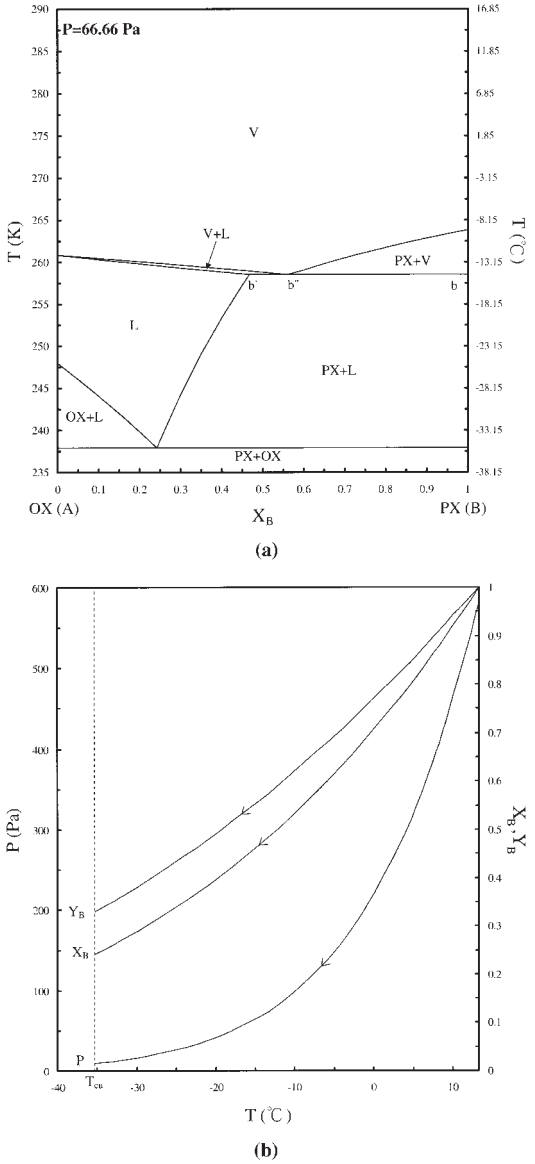


**Figure 1. (a) Phase diagram of OX and PX at $P$ = 66.66 Pa; (b) triple points of PX to simulate the path followed during the DF operation.**

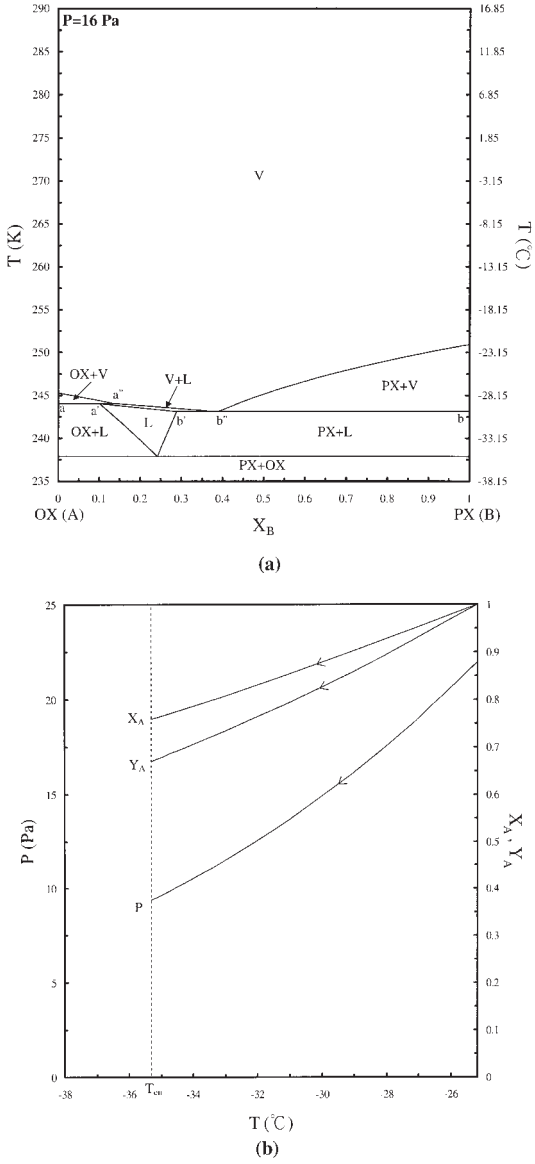


**Figure 2. (a) Phase diagram of OX and PX at $P$ = 16 Pa; (b) triple points of OX to simulate the path followed during the DF operation.**

For ideal liquid solutions, $\gamma_A \rightarrow 1$ and $\gamma_B \rightarrow 1$. At low pressures, $\phi_A \rightarrow 1$ and $\phi_B \rightarrow 1$. Thus, the variations of $P$, $X_A$, $X_B$, $Y_A$, and $Y_B$ with $T$ at a three-phase state can be determined by solving Eqs. 1–5. Figure 1b displays three curves—$P(T)$, $X_B(T)$, and $Y_B(T)$—to simulate the path followed during the DF operation in the production of PX crystals from the binary mixture. These curves show the starting and end points for any DF process applied at an initial given $X_B$ value.

To produce pure PX solid, the DF operable temperature range is from the triple-point temperature at an initial given $X_B$

**Table 1. Some Physical Properties for PX and OX***

| Property | PX | OX |
|---|---|---|
| Molecular weight | 106.167 | 106.167 |
| Boiling point, °C | 138.37 | 144.43 |
| Freezing point, °C | 13.26 | −25.17 |
| Triple point pressure, Pa (N/m$^2$) | 581.55 | 21.97 |
| Heat of melting, J/mol | $1.711 \times 10^4$ | $1.360 \times 10^4$ |

*From Kirk and Othmer, *Encyclopedia of Chemical Technology*.[2]

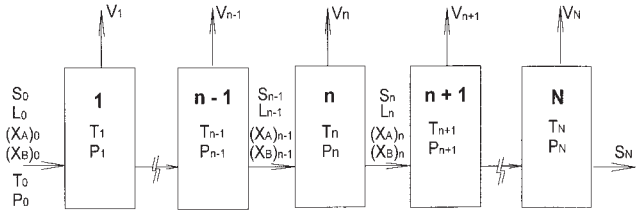


**Figure 3. Simulated DF operation where each stage is operated under an adiabatic condition at a three-phase equilibrium state.**

**Table 2. Simulation Results of DF Operation for a 200-g Liquid Feed of 90% PX and 10% OX ($\Delta T$ = 3°C)**

| Step | $P$ (Pa) | $T$ (°C) | $L$ (g) | $S$ (g) | $X_{PX}$ | $X_{OX}$ |
|---|---|---|---|---|---|---|
| 0 | 433.70 | 9.12 | 200 | 0 | 0.9 | 0.1 |
| 1 | 348.53 | 6.11 | 95.85 | 73.07 | 0.833 | 0.167 |
| 2 | 278.85 | 3.11 | 60.91 | 96.84 | 0.769 | 0.231 |
| 3 | 221.94 | 0.11 | 43.69 | 108.0 | 0.710 | 0.290 |
| 4 | 175.69 | −2.89 | 33.47 | 114.2 | 0.654 | 0.346 |
| 5 | 138.31 | −5.89 | 26.67 | 118.0 | 0.601 | 0.399 |
| 6 | 108.25 | −8.89 | 21.79 | 120.5 | 0.552 | 0.448 |
| 7 | 84.22 | −11.9 | 18.08 | 122.2 | 0.506 | 0.494 |
| 8 | 65.11 | −14.9 | 15.14 | 123.3 | 0.463 | 0.537 |
| 9 | 50.01 | −17.9 | 12.72 | 124.1 | 0.423 | 0.577 |
| 10 | 38.16 | −20.9 | 10.68 | 124.6 | 0.386 | 0.614 |
| 11 | 28.91 | −23.9 | 8.906 | 125.0 | 0.352 | 0.648 |
| 12 | 21.74 | −26.9 | 7.343 | 125.2 | 0.320 | 0.680 |
| 13 | 16.23 | −29.9 | 5.939 | 125.4 | 0.290 | 0.710 |
| 14 | 12.01 | −32.9 | 4.661 | 125.4 | 0.262 | 0.738 |
| 15 | 9.53 | −35.2 | 3.780 | 125.4 | 0.243 | 0.757 |

value to the eutectic temperature. For example, to produce PX crystals from the mixture of $X_B = 0.9$, the DF operable temperature range is from 9.12 to −35.3°C. The final DF operating temperature should be stopped above the eutectic temperature to avoid the cocrystallization of OX and PX. On the other hand, to produce PX crystals from the mixture of $X_B = 0.8$, the DF operable temperature range is from 4.63 to −35.3°C. Therefore, the DF operable temperature range decreases with decreasing $X_B$.

Figure 2a, which shows the existence of two three-phase states, illustrates the phase diagram of OX and PX at $P = 16$ Pa, which is lower than the triple-point pressure of pure OX. One is a three-phase state (point b, point b′, and point b″) having pure B-solid, and both liquid and vapor phases of mixtures at $T = 30.0$°C, $X_B = 0.29$, and $Y_B = 0.38$ on the right-hand side of the figure. The other is a three-phase state (point a, point a′, and point a″) having pure A-solid, and both liquid and vapor phases of mixtures at $T = 29.1$°C, $X_B = 0.10$, and $Y_B = 0.14$ on the left-hand side of the figure. Thus, the DF operation can be applied not only to produce PX crystals from the mixture in the range $0.24 < X_B < 1$, but also to produce OX crystals from the mixture in the range $0 < X_B < 0.24$.

When the DF operation is applied to produce OX crystals from the binary mixture in the range $0 < X_B < 0.24$, the DF process must always be maintained at a three-phase state having pure A-solid, and both liquid and vapor phases of mixtures. Thus, Eq. 1 should be replaced by

**Table 3. Comparison of Simulation and Experimental Results for a 200-g Liquid Feed of 90% PX and 10% OX**

| Feed | 1st DF ($T_f$ = −32.9°C, $P_f$ = 12.01 Pa) |
|---|---|
| 90% PX, 10% OX, 200 g | |
| Simulation results | 97.4% PX<br>130.1 g |
| Experimental results | 99.5% PX<br>118 g |
| Actual recovery rate of PX* | 65.6% |

*Actual recovery rate of PX = $\frac{\text{Final PX crystals by the DF experiments}}{\text{PX in the feed}}$

**Table 4. Simulation Results of DF Operation for a 200-g Liquid Feed of 85% PX and 15% OX ($\Delta T$ = 3°C)**

| Step | $P$ (Pa) | $T$ (°C) | $L$ (g) | $S$ (g) | $X_{PX}$ | $X_{OX}$ |
|---|---|---|---|---|---|---|
| 0 | 369.30 | 6.90 | 200 | 0 | 0.85 | 0.15 |
| 1 | 295.87 | 3.90 | 121.7 | 54.60 | 0.786 | 0.214 |
| 2 | 235.81 | 0.90 | 86.03 | 78.87 | 0.725 | 0.275 |
| 3 | 186.94 | −2.10 | 65.83 | 92.15 | 0.668 | 0.332 |
| 4 | 147.39 | −5.10 | 52.88 | 100.3 | 0.615 | 0.385 |
| 5 | 115.54 | −8.10 | 43.87 | 105.7 | 0.565 | 0.435 |
| 6 | 90.03 | −11.1 | 37.22 | 109.4 | 0.518 | 0.482 |
| 7 | 69.72 | −14.1 | 32.08 | 112.0 | 0.474 | 0.526 |
| 8 | 53.65 | −17.1 | 27.97 | 114.0 | 0.434 | 0.566 |
| 9 | 41.00 | −20.1 | 24.60 | 115.4 | 0.396 | 0.604 |
| 10 | 31.12 | −23.1 | 21.75 | 116.5 | 0.361 | 0.639 |
| 11 | 23.45 | −26.1 | 19.31 | 117.4 | 0.328 | 0.672 |
| 12 | 17.54 | −29.1 | 17.17 | 118.0 | 0.297 | 0.703 |
| 13 | 13.01 | −32.1 | 15.27 | 118.5 | 0.269 | 0.731 |
| 14 | 9.58 | −35.1 | 13.57 | 118.9 | 0.243 | 0.757 |

$$\ln[(X_A)(\gamma_A)] = \frac{\Delta H_{m,A}}{R}\left(\frac{1}{T_{m,A}} - \frac{1}{T}\right) + \frac{\Delta C_{P,A}}{R}\left(\frac{T_{m,A} - T}{T}\right) - \frac{\Delta C_{p,A}}{R}\ln\left(\frac{T_{m,A}}{T}\right) \quad (6)$$

Thus, the variations of $P$, $X_A$, $X_B$, $Y_A$, and $Y_B$ with $T$ at a three-phase state can be determined by solving Eqs. 2–6. Figure 2b displays three curves—$P(T)$, $X_A(T)$, and $Y_A(T)$—to simulate the path followed during the DF operation in the production of OX crystals from the binary mixture.

To produce pure OX solid, the DF operable temperature range is from the triple-point temperature at an initial given $X_A$ value to the eutectic temperature. For example, to produce OX crystals from the mixture of $X_A = 0.95$, the DF operable temperature range is from −27.1 to −35.3°C. Similarly, the final DF operating temperature should be stopped above the eutectic temperature. To produce OX crystals from the mixture of $X_A = 0.9$, the DF operable temperature range is from −29.1 to −35.3°C. Thus, the DF operable temperature range decreases with decreasing $X_A$.

Because the triple-point temperature of pure OX (−25.17°C) is much lower than that of pure PX (13.26°C), the DF operable temperature range for the separation of OX from the binary mixture is generally much smaller than that for the separation of PX. Therefore, it is expected that the separation of OX from the OX-enriched mixture in the DF operation is more difficult than the separation of PX from the PX-enriched mixture.

## DF Simulation Process

Because the DF process is conducted under an adiabatic condition at a three-phase equilibrium, the latent heat released

**Table 5. Comparison of Simulation and Experimental Results for a 200-g Liquid Feed of 85% PX and 15% OX**

| Feed | 1st DF ($T_f$ = −35.3°C, $P_f$ = 9.42 Pa) |
|---|---|
| 85% PX, 15% OX, 200 g | |
| Simulation results | 92.3% PX<br>132.4 g |
| Experimental results | 99.5% PX<br>111.7 g |
| Actual recovery rate of PX | 65.7% |

Table 6. Simulation Results of First DF Operation for a 200-g Liquid Feed of 95% OX and 5% PX ($\Delta T = 2$°C)

| Step | $P$ (Pa) | $T$ (°C) | $L$ (g) | $S$ (g) | $X_{OX}$ | $X_{PX}$ | |
|---|---|---|---|---|---|---|---|
| 0 | 18.84 | −27.1 | 200 | 0 | 0.95 | 0.05 | |
| 1 | 16.02 | −29.1 | 48.94 | 115.6 | 0.900 | 0.100 | |
| 2 | 13.55 | −31.1 | 23.87 | 134.1 | 0.852 | 0.148 | |
| 3 | 11.41 | −33.1 | 14.05 | 141.0 | 0.806 | 0.194 | |
| 4 | 9.57 | −35.1 | 8.821 | 144.3 | 0.762 | 0.238 | |
| 5 | 9.42 | −35.3 | 8.494 | 144.5 | 0.758 | 0.242 | End of 1st DF (Eutectic point) |

in forming B-solid (or A-solid) is removed by vaporizing portions of the A-component and the B-component. Thus, the DF process is simulated in a series of $N$ equilibrium-stage operations shown in Figure 3. Each stage is operated under an adiabatic condition at a three-phase equilibrium. The temperature of each stage is chosen to meet $T_n - T_{n-1} = \Delta T$ for $n = 1, 2, \ldots, N$. The vapor formed in each stage is condensed to the liquid and removed, whereas the solid and the liquid formed in each stage enter the next stage. The whole process starts from the liquid feed and continues until the liquid phase is completely eliminated.

When the DF operation is applied to produce B-solid from the binary liquid mixture in the range $0.24 < X_B < 1$, the DF process is operated at a three-phase state having pure B-solid, and both liquid and vapor phases of mixtures in each stage. The DF simulation equations are derived in the previous report by Shiau et al.[3]

On the other hand, when the DF operation is applied to produce A-solid from the binary liquid mixture in the range $0 < X_B < 0.24$, the DF simulation equations derived by Shiau et al.[3] need to be modified to account for the production of A-solid instead of B-solid. In other words, the DF process is operated at a three-phase state having pure A-solid, and both liquid and vapor phases of mixtures in each stage.

## Experimental

The experimental method is described in detail by Shiau et al.[3] At the start of the DF experiment, a 200-g mixture of OX and PX is injected into the vessel. The sample temperature drops nearly linearly from room temperature to −20°C in the first 100 min after the cooling jacket is circulated by the refrigerant. Then it drops very slowly from −20 to −35.3°C over the next 100 min. Typically, one DF experiment is completed within about 200 min. The whole DF experiment is stopped above the eutectic temperature ($T = -35.3$°C) to avoid the cocrystallization of OX and PX. The DF experiment is operated based on the simulated temperature and pressure. Therefore, because the sample temperature decreases during the DF operation, the operating pressure is reduced by controlling the vacuum pump.

## Results and Discussion

### *Separation of PX from the PX-enriched mixture*

The DF process can be applied to produce PX (B-component) crystals from the binary mixture in the range $0.24 < X_B < 1$. The simulation results for the separation of PX with a 200-g sample of $X_B = 0.9$ calculated by the simulation equations are listed in Table 2. The DF operating temperature and pressure are reduced from $T = 6.11$°C, $P = 348.53$ Pa in stage 1 to $T = -35.2$°C, $P = 9.53$ Pa in stage 15 during a series of 15 equilibrium-stage operations with $\Delta T = 3$°C. Note that the final DF operating temperature is stopped above the eutectic temperature. The DF experiments are performed based on the simulated temperature and pressure. The simulation and experimental results, compared in Table 3, indicate that, with a 200-g sample of $X_B = 0.9$, the experimental recovery is 118 g PX with 99.5% purity, as opposed to 130.1 g PX with 97.4% purity predicted from the simulation. The actual recovery rate of PX is 65.6% in one DF operation.

Similarly, the simulation results for the separation of PX with a 200-g sample of $X_B = 0.85$ are listed in Table 4. The simulation and experimental results are compared in Table 5, indicating that, with a 200-g sample of $X_B = 0.85$, the experimental recovery is 111.7 g PX with 99.5% purity, as opposed to 132.3 g PX with 92.3% purity predicted from the simulation. The actual recovery rate of PX is 65.7% in one DF operation. Thus, in the above two cases, the DF experiments both lead to less recovery of PX with higher purity compared to the DF simulation.

### *Separation of OX from the OX-enriched mixture*

The DF process can be applied to produce OX (A-component) crystals from the binary mixture in the range $0 < X_B < 0.24$ (that is, $0.76 < X_A < 1$). The simulation results for the separation of OX with a 200-g sample of $X_B = 0.05$ (that is, $X_A$

Table 7. Simulation Results of Second DF Operation for a 200-g Liquid Feed of 95% OX and 5% PX ($\Delta T = 1.5$°C)

| Step | $P$ (Pa) | $T$ (°C) | $L$ (g) | $S$ (g) | $X_{OX}$ | $X_{PX}$ | |
|---|---|---|---|---|---|---|---|
| 0 | 20.10 | −26.3 | 200 | 0 | 0.969 | 0.031 | |
| 1 | 17.74 | −27.8 | 32.62 | 128.4 | 0.931 | 0.069 | |
| 2 | 15.68 | −29.3 | 14.43 | 141.8 | 0.894 | 0.106 | |
| 3 | 13.83 | −30.8 | 7.851 | 146.4 | 0.858 | 0.142 | |
| 4 | 12.17 | −32.3 | 4.442 | 148.4 | 0.823 | 0.177 | |
| 5 | 10.68 | −33.8 | 2.302 | 149.5 | 0.789 | 0.211 | |
| 6 | 9.42 | −35.3 | 0.866 | 150.1 | 0.758 | 0.242 | End of 2nd DF (Eutectic point) |

Table 8. Simulation Results of Third DF Operation for a 200-g Liquid Feed of 95% OX and 5% PX ($\Delta T$ = 1°C)

| Step | $P$ (Pa) | $T$ (°C) | $L$ (g) | $S$ (g) | $X_{OX}$ | $X_{PX}$ | |
|---|---|---|---|---|---|---|---|
| 0 | 20.74 | −25.9 | 200 | 0 | 0.981 | 0.019 | |
| 1 | 19.16 | −26.9 | 25.39 | 134.2 | 0.955 | 0.045 | |
| 2 | 17.67 | −27.9 | 10.81 | 145.0 | 0.930 | 0.070 | |
| 3 | 16.28 | −28.9 | 5.786 | 148.5 | 0.905 | 0.095 | |
| 4 | 14.99 | −29.9 | 3.240 | 150.1 | 0.880 | 0.120 | |
| 5 | 13.78 | −30.9 | 1.667 | 151.0 | 0.856 | 0.144 | |
| 6 | 12.65 | −31.9 | 0.563 | 151.5 | 0.833 | 0.167 | |
| 7 | 11.95 | −32.6 | 0.001 | 151.6 | 0.818 | 0.182 | End of 3rd DF |

= 0.95) calculated by the simulation equations are listed in Table 6. The DF operating temperature and pressure is reduced from $T = -29.1$°C, $P = 16.02$ Pa in stage 1 to $T = -35.3$°C, $P = 9.42$ Pa in stage 5 during a series of five equilibrium stage operations with $\Delta T = 2$°C. These DF operating temperature and pressure ranges in the separation of OX from the OX-enriched mixture are much smaller than those in the separation of PX from the PX-enriched mixture.

In the first DF experiment, it is found that the purity of OX product increases from 95 to only 96.9%; the second DF experiment is further applied. In practice, the final solid product obtained from the first DF is completely dissolved and used as a new feed for the second DF experiment. If the final product consists of the solid and the liquid, the solid is completely dissolved and mixed with the liquid. Then, the product is weighed and analyzed by gas chromatography (GC) for the composition. Accordingly, the subsequent DF simulation is performed. Thus, consecutive DF experiments are applied to increase the purity of OX product.

Simulations for the consecutive DF operations are listed in Tables 6–9. The simulation and experimental results, compared in Table 10, indicate that, with a 200-g sample of $X_A = 0.95$, the experimental recovery is 168.6 g OX with 96.9% purity after the first DF, as opposed to 153.0 g PX with 98.7% purity predicted from the simulation. Although the purity predicted from the simulation can reach 99.9% after the second DF, the actual DF experiments can raise the purity to only 99.1% after the fourth DF. Thus, as seen in Table 10, the DF experiments lead to slightly more recovery of OX with lower purity compared to the DF simulation. The actual recovery rate of OX is only 55.1% during the four DF operations.

## Conclusions

In the actual DF experiments, there are some deviations from the ideal DF simulations:

(1) The ideal assumption of unity activity and fugacity coefficient might not be followed.

(2) The three-phase equilibrium condition might not be always attained during the temperature- and pressure-reducing processes.

(3) It is difficult to perform the experiments under an absolutely adiabatic condition.

(4) The temperature of the liquid sample is not uniformly distributed during the temperature-reducing process because no stirring was applied in the sample vessel.

(5) The pressure of the liquid sample is influenced by the liquid hydraulic pressure.

(6) Because of the similar structures of PX and OX, one component might be incorporated into the crystal lattice of the other component, leading to the presence of impurity in the final crystals. Besides, liquid inclusion is also a possible source for the presence of impurity in crystal growth.

However, the DF simulations can still provide essential information in operation of the actual DF process. The DF experimental results are in substantial agreement with the DF simulations.

As explained earlier, the DF operable temperature and pressure ranges in the separation of OX from the OX-enriched mixture ($0 < X_B < 0.24$) are generally smaller than those in the separation of PX from the PX-enriched mixture ($0.24 < X_B < 1$). Therefore, it is expected that the separation of OX from the mixture is more difficult than the separation of PX from the mixture. It is confirmed by the DF experiments that only one DF process is required to purify PX in the PX-enriched mixture from 90 to 99.5% or even from 85 to 99.5%. On the other hand, four DF operations are required to purify OX in the OX-enriched mixture from 95 to 99.1%.

In conventional crystallization, filtration or centrifugation is needed to separate the solid crystals from the mother liquor. Then the crystalline mass is purified by a partial melting of the crystals to wash out adhering impurities on the crystal surfaces. However, the DF process is continued until the liquid phase is completely eliminated and only the pure crystals remain in the feed. The low-pressure vapor formed in the process is condensed and removed. Subsequently, filtration or centrifugation is not needed because no mother liquor is present with the pure crystals. In addition, crystal washing is not required because only the pure solid crystals remain in the feed and no impurities are adhered on the crystal surfaces at the end of the operation. However, the design of industrial-scale DF equipment is a

Table 9. Simulation Results of Fourth DF Operation for a 200-g Liquid Feed of 95% OX and 5% PX ($\Delta T$ = 0.8°C)

| Step | $P$ (Pa) | $T$ (°C) | $L$ (g) | $S$ (g) | $X_{OX}$ | $X_{PX}$ | |
|---|---|---|---|---|---|---|---|
| 0 | 21.24 | −25.6 | 200 | 0 | 0.988 | 0.012 | |
| 1 | 19.88 | −26.4 | 8.792 | 147.1 | 0.967 | 0.033 | |
| 2 | 18.64 | −27.2 | 3.056 | 151.2 | 0.946 | 0.054 | |
| 3 | 17.47 | −28.0 | 1.144 | 152.4 | 0.926 | 0.074 | |
| 4 | 16.36 | −28.8 | 0.134 | 152.8 | 0.906 | 0.094 | |
| 5 | 16.16 | −29.0 | 0.006 | 152.9 | 0.902 | 0.098 | End of 4th DF |

**Table 10. Comparison of Simulation and Experimental Results for a 200-g Liquid Feed of 95% OX and 5% PX**

| Feed | 1st DF ($T_f$ = −35.3°C, $P_f$ = 9.42 Pa) | 2nd DF ($T_f$ = −35.3°C, $P_f$ = 9.42 Pa) | 3rd DF ($T_f$ = −32.6°C, $P_f$ = 11.95 Pa) | 4th DF ($T_f$ = −29.0°C, $P_f$ = 16.16 Pa) |
|---|---|---|---|---|
| 95% OX, 5% PX, 200 g | | | | |
| Simulation results | 98.7% OX | 99.9% OX | 100% OX | 100% OX |
| | 153.0 g | 127.3 g | 108.7 g | 103.0 g |
| Experimental results | 96.9% OX | 98.1% OX | 98.8% OX | 99.1% OX |
| | 168.6 g | 143.4 g | 134.7 g | 104.7 g |
| Actual recovery rate of OX* | 88.7% | 75.5% | 70.9% | 55.1% |

*Actual recovery rate of OX = $\frac{\text{Final OX crystals by the DF experiments}}{\text{OX in the feed}}$

challenging problem because an efficient DF process is required to provide the liquid mixture with a large exposure surface area available for simultaneous vaporization and crystallization during a series of three-phase equilibrium stages at reduced temperature and pressure.

## Acknowledgments

Financial support of the National Science Council of the Republic of China is gratefully acknowledged.

## Notation

$\Delta C_{p,j}$ = change in the heat capacity from solid phase to liquid phase for the $j$th component
$\Delta H_{m,j}$ = change in the enthalpy from solid phase to liquid phase for the $j$th component
$L_n$ = mass flow rate of the liquid phase out of stage $n$
$P$ = pressure
$P_j^{sat}$ = saturated pressure of liquid of the $j$th component
$R$ = ideal gas constant
$S_n$ = mass flow rate of the solid phase out of stage $n$
$T$ = temperature
$T_{eu}$ = eutectic temperature
$T_{m,j}$ = melting temperature of the $j$th component
$V_n$ = mass flow rate of the vapor phase out of stage $n$
$X_j$ = composition of the $j$th component of the liquid phase
$Y_j$ = composition of the $j$th component of the vapor phase

### *Greek letters*

$\gamma_j$ = activity coefficient of the $j$th component in the liquid phase
$\phi_j$ = fugacity coefficient of the $j$th component in the vapor phase

### *Subscripts*

0 = in the feed
$n$ = in stage $n$
$f$ = in the final operation

## Literature Cited

1. Cheng CY, Cheng SW. *Distillative Freezing Process for Separating Volatile Mixtures and Apparatuses for Use Therein*. U.S. Patent No. 4 218 893; 1980.
2. Kirk RE, Othmer DF, eds. *Encyclopedia of Chemical Technology*. Vol. 4. New York, NY: Wiley; 1991.
3. Shiau LD, Wen CC, Lin BS. Separation and purification of *p*-xylene from the mixture of *m*-xylene and *p*-xylene by distillative freezing. *Ind Eng Chem Res.* 2005;44:2258-2265.
4. Prausnitz JM, Lichtenthaler RN, de Azevedo EG. *Molecular Thermodynamics of Fluid-Phase Equilibria*. Upper Saddle River, NJ: Prentice-Hall; 1999.
5. Smith JM, Van Ness HC, Abbott MM. *Introduction to Chemical Engineering Thermodynamics*. Singapore: McGraw-Hill; 2001.

*Manuscript received Jun. 27, 2005, and revision received Dec. 15, 2005.*